

Joint Optimization of Scheduling and Power Control in Wireless Networks: Multi-Dimensional Modeling and Decomposition

Lu Liu¹, Member, IEEE, Yu Cheng¹, Senior Member, IEEE, Xianghui Cao¹, Senior Member, IEEE, Sheng Zhou¹, Member, IEEE, Zhisheng Niu¹, Fellow, IEEE, and Ping Wang², Senior Member, IEEE

Abstract—The energy efficiency of future networks is becoming a significant and urgent issue, calling for greener network designs. However, the increasing complexity in network structure and resource space lead to growing problem scales and coupled resource dimensions, which bring great challenges in obtaining a joint solution in optimizing the energy efficiency. In this paper, we develop a multi-dimensional network model on the basis of tuple-links associated with transmission patterns (TPs) and formulate the optimization problem as a TP based scheduling problem which jointly solves transmission scheduling, routing, power control, radio, and channel assignment. In order to tackle the complexity issues, we propose a novel algorithm by exploiting the delay column generation technique to decompose the coupled problem into recursively solving a master problem for scheduling and a sub-problem for power allocation. Further, we theoretically prove that the performance gap between the proposed algorithm and the optimum is upper bounded by that for the sub-problem solution, where the latter is derived by solving a relaxed version of the sub-problem. Numerical results demonstrate the effectiveness of the multi-dimensional framework and the benefit of the proposed joint optimization in improving network energy efficiency.

Index Terms—Multi-radio multi-channel networks, optimization, resource allocation, energy efficiency

1 INTRODUCTION

ENERGY efficiency of next generation wireless networks is a critical and urgent issue. The key to improving energy efficiency of wireless networks relies on configuring and allocating various network resources in temporal, spatial, spectral and power dimensions in terms of routing, link scheduling, channel allocation and power control. Generally, different network resources are coupled such that they cannot be determined independently for optimal performance, which demands a joint optimization solution. What's more, in order to meet the rapidly growing traffic demands, wireless networks are evolving into more and more complex structures and hence large scales of joint optimization problems. Obtaining a joint optimization solution over wireless networks becomes a challenging issue, which motivated us to develop more efficient solutions.

Many wireless networks can be abstracted as that each network node has multiple radio interfaces operating on

multiple available wireless channels, yielding the generic multi-radio multi-channel (MR-MC) network model with multi-dimensional resource space [1], [2], [3]. With this model for the joint optimization problem, the optimization variable can be viewed as a compound of multiple resource allocation strategies, including selection of transmitters and receivers for transmission links, radio and channel assignment, transmit power control, routing and link scheduling.

The existing studies on energy-efficient networking in MR-MC wireless networks have addressed the joint optimization issues over different dimensions, but a generic joint optimization solution over the whole multi-dimensional space (especially when power control is involved) is still not available, to the best of our knowledge. Radio/channel assignment and transmission scheduling in MR-MC wireless networks have been studied with the objective to maximize network capacity [4], [5], [6], [7]. Specifically, protocol interference model is widely adopted to characterize the interferences among links as a conflict graph, over which independent set based scheduling is then used to facilitate a linear programming (LP) based formulation [8], [9], [10]. However, such a model simplifies transmission links to be either deactivated or activated with fixed transmit power, which can neither model dynamic power assignment nor accurately reflect the practical interference magnitude. The more realistic signal-to-interference-plus-noise ratio (SINR) based physical interference model can model transmission interferences under the power control. Link scheduling for capacity optimization under the physical interference model has been studied in [11], [12], [13], but is limited to single-channel scenarios. How to incorporate physical interference model based power control into multi-dimensional resource

- L. Liu and Y. Cheng are with the Department of Electrical and Computer Engineering, Illinois Institute of Technology, Chicago, IL 60616. E-mail: lliu41@hawk.iit.edu, cheng@iit.edu.
- X. Cao is with the School of Automation, Southeast University, Nanjing 210096, China. E-mail: xh.cao@ieee.org.
- S. Zhou and Z. Niu are with the Tsinghua National Laboratory for Information Science and Technology, Tsinghua University, Beijing 100084, China. E-mail: {sheng.zhou, niuzhs}@tsinghua.edu.cn.
- P. Wang is with the School of Computer Engineering, Nanyang Technological University, Singapore 639798. E-mail: wangping@ntu.edu.sg.

Manuscript received 31 May 2017; revised 14 Feb. 2018; accepted 20 July 2018. Date of publication 1 Aug. 2018; date of current version 31 May 2019.

(Corresponding author: Yu Cheng.)

For information on obtaining reprints of this article, please send e-mail to: reprints@ieee.org, and reference the Digital Object Identifier below.

Digital Object Identifier no. 10.1109/TMC.2018.2861859

space so as to provide energy-efficient joint scheduling and power control solution remains a challenging issue.

It has been known that the optimal transmission scheduling problem in wireless networks is NP hard [14], [15], [16], [17], let alone the more complicated problem of energy-efficient joint scheduling and power control. To this end, we apply the tuple-link based multi-dimensional network model [6], with which the joint allocation over multi-dimensional resource space is reduced to the scheduling of tuple-links. Further, we propose a new concept of *transmission pattern* (TP) which integrates both scheduling and power control to facilitate LP formulation of the joint optimization problem. A TP is defined as a vector of transmit power assignment of all the tuple-links in the network. In a TP, the SINR at the receiver of each tuple-link can be calculated based on the power allocation of all the tuple-links so that the transmission capacity of the tuple-link can be determined according to the Shannon-Hartley equation. Therefore, a TP characterizes a possible transmission state in the network, including the resource allocation information across all the dimensions. By considering discretized transmit power levels, the joint scheduling and power assignment problem in the multi-dimensional resource space can be ultimately transformed into a scheduling problem of a finite number of TPs, which facilitates an LP formulation. This TP based scheduling problem is formulated in a similar manner as that of independent set based scheduling [3], [6], but is compatible with physical interference model and flexible power allocation. The solution to the TP based optimization provides joint scheduling and power control, as well as the resource allocation on all the other resource dimensions.

The TP based scheduling transforms the NP hardness into an extremely large problem scale due to exponentially many possible patterns, thus exponentially many decision variables. We then exploit a decomposition based approach by leveraging delay column generation (DCG), which starts with an initial subset of TPs and then gradually adding new TPs that can improve the objective value. The DCG based method repeatedly solves a master problem and a sub-problem, where the master problem performs scheduling on existing TPs and the sub-problem searches for a new entering TP by solving a maximum utility problem. We further reveal that the sub-problem is indeed to find the most energy-efficient TP according to the information extracted from the existing TPs, and show that it is equivalent to finding the optimal power allocation over tuple-links. Thus the joint optimization problem is decomposed into an iterative procedure combining scheduling phase and power control phase, while optimality remains intact during the decomposition.

As solving the sub-problem still incurs high computational complexity in searching over the entire TP space, we further propose a greedy algorithm to solve the sub-problem efficiently. Moreover, through theoretical analysis, we prove that the performance gap between the achieved and optimal solutions is upper bounded by the gap achieved in solving the sub-problem, which can be derived by solving a relaxed sub-problem.

Some preliminary results appeared in [18] focused on the simple single-hop scenario where per-link traffic demand was explicitly specified in the optimization formulation. This paper extends the framework to generic multi-hop scenarios with multiple commodity flows. The obtained joint solution further provides routing information in a way that

the source to destination paths for each commodity flow are implied by the obtained schedule of the links. In addition, a new modeling method and the concept of interference coefficient is introduced in this paper which seamlessly integrates radio conflict and co-channel interference. Further, in solving the sub-problem, a greedy algorithm is proposed in this paper instead of the learning based algorithm in [18] for higher computational efficiency.

The main contributions of this paper are as follows:

- 1) We transform the joint scheduling and power control problem for wireless network energy efficiency optimization in the multi-dimensional resource space into a TP based scheduling problem and formulate it as an LP.
- 2) To solve the large-scale TP scheduling problem, we exploit a decomposition approach by leveraging the DCG technique that decomposes the optimization problem into scheduling (master problem) and energy-efficient TP selection (sub-problem), and reveal the physical meaning of the decomposition. Further, we propose a greedy algorithm to efficiently solve the NP hard sub-problem.
- 3) We theoretically prove that the performance gap of the original problem's solution is bounded by that of the sub-problem, and derive the latter by formulating and solving a relaxed version of the sub-problem.
- 4) We present numerical results to demonstrate the energy efficiency improvement of joint scheduling and power control, and analyze how the allocations of multi-dimensional resources affect the energy efficiency in the network.

The remainder of this paper is organized as follows. Section 2 reviews more related work. Section 3 describes the system model and problem formulation. Section 4 presents the decomposition framework and algorithm, with the performance bound of the proposed algorithm analyzed in Section 5. Section 6 presents numerical results, and Section 7 gives the conclusion remarks.

Notations. Throughout this paper, we use $|\mathcal{A}|$ to denote the size of set \mathcal{A} . Boldfaced capital letters are used to denote matrices, while boldfaced lower-case letters are used to denote vectors. All the vectors are column vectors by default, and the transpose of a matrix \mathbf{A} is denoted as \mathbf{A}^T . Table 1 summarizes the main notations used in this paper.

2 RELATED WORK

Energy-efficient wireless networking has gained great attention in the literature, especially for networks with multi-dimensional resource space such as heterogeneous networks [19], cognitive radio networks [20], [21], [22] and networks with device-to-device communications [23], [24]. Resource allocation for heterogeneous cognitive radio network is studied in [19], where a Stackelberg game approach is adopted with gradient based iteration algorithm as a solution. Channel assignment and power control are investigated in [20] which aims to maximize energy efficiency of cognitive radio networks and maps the optimization problem to a maximum matching problem. Similarly, a joint solution of channel and power allocation is proposed in [21], with the objective of maximizing overall network throughput. In that paper, physical interference model is applied and the problem is solved by formulating a

TABLE 1
Notations

\mathcal{N}	node set
\mathcal{C}	set of channels
$\mathcal{R}, \mathcal{R}_v$	radio set, radio set of node v
\mathcal{P}	set of available power levels
λ	flow commodity
$q^{(\lambda)}$	demand of commodity λ
l, \mathcal{L}	tuple-link, set of all tuple-links
γ_l	SINR of tuple-link l
g_{lm}	generalized interference coefficient between l and m
α, \mathcal{A}	TP, set of all TPs
t_α	portion of transmission time assigned to TP α
$p_{l,\alpha}, r_{l,\alpha}$	transmit power, capacity of link l achieved in TP α
u, U, \bar{u}	link utility, system utility, utopian utility

bargaining based cooperative game. The work in [22] investigates the joint optimization of spectrum and energy efficiency in cognitive networks with power and subchannel allocation, where the authors propose a tradeoff metric based problem transformation and exploiting convex problem structure. In [23], an energy efficiency maximization problem is formulated as a non-convex program, which is then transformed into a convex optimization problem with nonlinear fractional programming. The authors in [24] consider joint radio and power allocation for energy efficiency optimization, and develop an auction game based approach. The above works focus on specific network scenarios or configurations, which could not be applied to generic MR-MC networks with multi-dimensional resource spaces. Furthermore, as most of them focus on channel and power allocation, joint optimizations incorporating link scheduling has not been well studied.

In [25], the problem of energy efficiency optimization in MR-MC networks is considered to derive radio/channel assignment and scheduling solutions for optimal energy efficiency under the requirement of full network capacity. A similar approach is adopted in [26] to minimize energy consumption with guaranteed capacity requirement. The problem is solved with a decomposed approach due to the large scale solution space. While these works take protocol interference model to simplify the scheduling problem, the more realistic physical interference model is applied in [27] for a joint scheduling and radio configuration problem. However, power control is not accounted, i.e., they all use fixed transmit power in the formulation.

To take power allocation into resource allocation, the authors in [28] propose an algorithm to jointly allocate channel and power with a utility based learning method in a decentralized manner. The utility is characterized by the transmission rate achieved by links and the solution can maximize the sum rate of links, but without considering energy cost. For energy efficiency optimization, a joint cell selection and power allocation problem for heterogeneous networks is formulated in [29] and solved with a Lagrange dual based method, where the proposed model does not apply to generic multi-dimensional resource space. The work in [30] proposes a two-step approach which first fixes transmit power to solve for scheduling and then optimizes the transmit power on the solved scheduling solution. However, such a decomposition will lead to sub-optimality since scheduling and power control are indeed solved separately. A joint solution of scheduling, channel allocation and power control is proposed in [31], but the achievable data rate on

links is assumed constant. This model cannot fully reflect the link capability, since the latter is characterized by the real-time SINR at the receiver. In sum, in the literature, a joint optimization solution towards energy efficient networking over the multi-dimensional resource space including routing, link scheduling, radio/channel assignment and power allocation has not been fully investigated, which is then to be studied in this paper.

3 PROBLEM FORMULATION

3.1 Network Model

Consider a generic MR-MC network with node set \mathcal{N} . Each node $v \in \mathcal{N}$ is equipped with one or multiple radio interfaces which are denoted as radio set \mathcal{R}_v . Define the set of all radios in the network as \mathcal{R} , thus $\mathcal{R} = \cup_{v \in \mathcal{N}} \mathcal{R}_v$. For each radio, all the other nodes' radios within its maximum transmission range are defined as its neighbors. For a non-isolated node, each of its radios can set up transmission links to all its neighbors. Denote the maximum transmit power of a radio as p_{\max} , and assume that the transmit power of each radio takes value from a discrete set of power levels \mathcal{P} . There is a number of non-overlapping channels available to each radio. We denote all the channels as set \mathcal{C} . We consider a slot-based model, which means the network is static within a time slot such that all the network parameters remain unchanged during this slot.

The objective is to minimize the total energy consumption in the network under traffic demand requirement. Denote the set of multiple commodity flows as $\{1, \dots, \lambda, \dots, \Lambda\}$. Each flow λ is specified by its corresponding source-destination node pair and flow demand. Therefore, it requires to jointly address: routing, link scheduling, radio and channel assignments, and transmit power control. In this optimization, the scheduling problem is to select transmission links and decide the transmission time for them. It can be seen that the joint optimization problem involves both continuous and discrete decision variables, making it a mixed-integer problem which is known of high complexity. In what follows, we present a tuple-link based framework to remodel the network, which facilitates an LP formulation and problem decomposition.

A *tuple-link* is defined as a combined resource allocation for a transmission indicating the transmitter radio, the receiver radio¹ and the operating channel [3]. Denote \mathcal{L} as the set of all the tuple-links in the network. Tuple-link only exists when there exists a corresponding physical link (between a radio and its neighbor); a physical link can be mapped to multiple tuple-links. Fig. 1 gives an example of tuple-links between two nodes, where Node 1 has two radios, Node 2 has one radio, and 2 channels are available. As shown by the dash lines, there exist 8 tuple-links specified by different transmitters, receivers or channels.

With this tuple-link based framework, the above optimization problem becomes to jointly solve scheduling and power control of the tuple-links since radio and channel assignment is encapsulated into tuple-link selection. In the rest of this paper, we use "link" to stand for "tuple-link" unless stated otherwise.

In a wireless network, links may suffer from interference from other concurrent transmitting links. In this paper, we

1. Tuple-link is directional since the transmitter and receiver are specified.

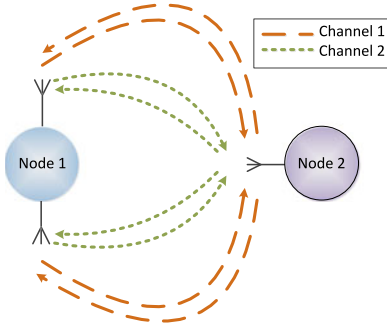


Fig. 1. Tuple-link example.

consider physical interference model, in which the capacity of a link can be characterized by the SINR at the receiver. For a link $l \in \mathcal{L}$, the received SINR is defined as

$$\gamma_l = \frac{g_l p_l}{I_l + \sigma^2} = \frac{g_l p_l}{\sum_{m \in \mathcal{L} \setminus l} g_m p_m + \sigma^2}, \quad (1)$$

where g_l , p_l , I_l , σ^2 denote the link gain, transmit power, received interference and the noise power, respectively. Particularly, g_{ml} is used to characterize the strength of interference from m to l , to be discussed in details in the following. The capacity (maximum achievable transmission rate) of link l can be expressed as

$$r_l = B_l \log_2(1 + \gamma_l), \quad (2)$$

where B_l is the corresponding channel bandwidth of l .

The link gain of l is given as $g_l = \rho(d_l)$, where d_l is the distance between l 's transmitter and receiver and $\rho(\cdot)$ is a function of d_l (e.g., the path loss function). Similarly, $g_{ml} = \rho(d_{ml})$ if l and m transmit in the same channel with d_{ml} as the distance from m 's transmitter to l 's receiver. Notice that two links on different channels will not generate co-channel interference to each other and in this case $g_{ml} = 0$. Besides co-channel interference, two links may not work simultaneously due to radio conflict. For example, two links cannot share the same transmitter radio for simultaneous transmissions. The radio conflict is usually expressed as integer constraints in optimization problems [27], [31] or considered separately aside from other resource allocation [18]. In order to facilitate linear programming, we extend the definition of g_{ml} to cover the radio conflict relationship, and specifically redefine it as *interference coefficient*. We apply a very large interference coefficient between links sharing the same radio. For example, if l and m have the same transmitter radio, then we may set $g_{ml} = \infty$. Assume all the radios in the network are half-duplex, and at any time a radio interface can be occupied by at most one link for transmission. In this case, the interference coefficient can be defined as

$$g_{ml} \triangleq \begin{cases} \rho(d_{ml}), & \text{if } l \text{ and } m \text{ use different radios} \\ & \text{and are on the same channel;} \\ 0, & \text{if } l \text{ and } m \text{ use different radios} \\ & \text{and are on different channels;} \\ \infty, & \text{if } l \text{ and } m \text{ share one or two radios.} \end{cases}$$

where ∞ stands for a significantly large number. According to this definition, the SINR expression in (1) is able to characterize both the radio conflict and interference, thus the

optimization problem can be formulated without additional radio constraints.²

3.2 Optimization Problem Formulation

Considering the conflicting objectives of throughput enhancement and energy saving, we will take a multi-objective optimization approach, which is to keep one objective and transform the other one to constraint [26], [32], [33]. Particularly, the energy efficiency is optimized by minimizing the total energy consumption in the network while satisfying flow demands of multiple commodities.

Suppose the demand of commodity flow λ is $q^{(\lambda)}$. To specify the source and destination of each flow, define demand vector $\mathbf{q}^{(\lambda)} = (q_1^{(\lambda)}, \dots, q_{|\mathcal{N}|}^{(\lambda)})'$ as

$$q_i^{(\lambda)} \triangleq \begin{cases} q^{(\lambda)}, & \text{if } i \text{ is the source node of flow } \lambda \\ -q^{(\lambda)}, & \text{if } i \text{ is the destination node of flow } \lambda \\ 0, & \text{otherwise.} \end{cases}$$

Denote $f_l^{(\lambda)}$ as flow rate for commodity λ on link l , then $\mathbf{f}^{(\lambda)} = (f_1^{(\lambda)}, \dots, f_{|\mathcal{L}|}^{(\lambda)})'$ is the flow vector of commodity λ on all the links. Since flow rate is defined for each link, it can be related to nodes with an $|\mathcal{N}|$ by $|\mathcal{L}|$ node-flow incident matrix \mathbf{H} , whose entries are defined as

$$h_{ij} \triangleq \begin{cases} 1, & \text{if link } j \text{ carries outgoing flow from node } i \\ -1, & \text{if link } j \text{ carries incoming flow to node } i \\ 0, & \text{otherwise.} \end{cases}$$

Based on the above definition, the flow balance constraints for each commodity can be expressed as

$$\mathbf{H}\mathbf{f}^{(\lambda)} = \mathbf{q}^{(\lambda)}, \quad \lambda = 1, \dots, \Lambda. \quad (3)$$

Generally, a link may use different transmit power at different time such that the mutual interference among links can be dynamically coordinated and the transmission rate can be adjusted. At a time instance, the transmit power levels of all the tuple-links form a *transmission pattern*. A TP implies the transmission state of all the links in the network, including which radios and channels are being used as well as the corresponding transmit power and link capacity. Recall that the scheduling problem we defined is to decide when and how long the links should transmit such that the flow demands can be satisfied with minimum energy consumption. Therefore, with the concept of TP introduced, the problem of joint scheduling and power control becomes to select TPs and decide transmission time for them.

Since the sets of links and transmit power levels are finite, the total number of possible TPs is finite. In each TP, if a link is assigned a non-zero transmit power level, the tuple-link is considered to be *active*. Let \mathcal{A} be the set of all TPs in the network. Denote the portion of transmission time assigned to pattern α as t_α . Let the transmit power and the capacity of link l achieved in pattern α be $p_{l,\alpha}$ and $r_{l,\alpha}$, respectively. Since each TP defines the transmit power levels of all links, $r_{l,\alpha}$ can be expressed as a function of $p_{l,\alpha}$, which is

2. The generalized radio conflict model can adapt to other network scenarios that have different types of radio constraints by correspondingly adjusting the values in the definition.

$$r_{l,\alpha} = B_l \log_2 \left(1 + \frac{g_l p_{l,\alpha}}{\sum_{m \in \mathcal{L} \setminus l} g_m p_{m,\alpha} + \sigma^2} \right). \quad (4)$$

Accordingly, the total traffic rate (including all commodities) on link l is bounded as

$$f_l = \sum_{\lambda \in \Lambda} f_l^{(\lambda)} \leq \sum_{\alpha \in \mathcal{A}} r_{l,\alpha} t_\alpha, \quad \forall l \in \mathcal{L} \quad (5)$$

$$\sum_{\alpha \in \mathcal{A}} t_\alpha = 1. \quad (6)$$

Thus, the energy-efficient resource allocation problem can be formulated as a TP based scheduling problem to minimize power consumption while satisfying flow demand, i.e.,

Problem 1 (Original optimization problem).

$$\min_{\{f_l^{(\lambda)}, t_\alpha\}} E = \sum_{\alpha \in \mathcal{A}} \sum_{l \in \mathcal{L}} p_{l,\alpha} t_\alpha \quad (7)$$

$$s.t. \quad \text{constraints (3), (4), (5), (6)} \quad (8)$$

$$f_l^{(\lambda)} \geq 0, \quad \forall l \in \mathcal{L}, \quad \lambda = 1, \dots, \Lambda$$

$$t_\alpha \geq 0, \quad \forall \alpha \in \mathcal{A}. \quad (9)$$

The optimization variables are flow variables $f_l^{(\lambda)}$, as well as transmission time portion t_α assigned to TPs. The objective function in (7) stands for the total power consumption which is the summation of power consumption over all the links in all TPs.

Lemma 1. In the optimal solution of Problem 1, constraint (5) will reach equality.

Proof. The lemma can be proved by contradiction. Suppose with the optimal solution, constraint (5) does not reach equality, i.e., there exists a link l such that $f_l < \sum_{\alpha \in \mathcal{A}} r_{l,\alpha} t_\alpha$. We call such a link over-scheduled, which indicates some pattern is providing more than necessary capacity to link l . Since f_l is non-negative, there must exist a pattern α_1 with $r_{l,\alpha_1} t_{\alpha_1} > 0$ ($p_{l,\alpha_1} > 0$).

Then, we look for a pattern α_2 that has smaller capacity on l but no lower rate on the other links. In other words, α_2 should satisfy $0 \leq r_{l,\alpha_2} < r_{l,\alpha_1}$ and $r_{m,\alpha_2} \geq r_{m,\alpha_1}, \forall m \neq l$. It can be seen that any pattern with a lower power level on l and same levels on the other links applies. Since $p_{l,\alpha_1} > 0$, we can always find such patterns. Notice that α_2 has less power consumption than α_1 .

The equality on link l can be achieved by removing the over-scheduled capacity on link l , which can be done by moving part of the traffic load from α_1 to α_2 . In other words, the equality can be achieved by designing a new schedule that moves a portion of t_{α_1} to t_{α_2} . Such a new schedule $\{t'_\alpha\}$ can be obtained by solving

$$t'_{\alpha_1} + t'_{\alpha_2} = t_{\alpha_1} + t_{\alpha_2} \quad (10)$$

$$t'_\alpha = t_\alpha, \forall \alpha \in \mathcal{A} \setminus \{\alpha_1, \alpha_2\} \quad (11)$$

$$f_l = \sum_{\alpha \in \mathcal{A}} r_{l,\alpha} t'_\alpha. \quad (12)$$

Under the new schedule, the capacity of other links will not be reduced while the inequality on link l will become equality, which means (5) still holds and the new schedule is a feasible solution.

Since part of the transmission time of pattern α_1 is re-scheduled to pattern α_2 while the latter has less power consumption, the new solution will consume less power compared to the original one, which means the original solution is not optimal and contradicts the assumption. This completes the proof.³ \square

Then, with all the constraints in equality, we can rewrite the optimization problem into standard matrix form as follows:

Problem 1 (Original problem in matrix form).

$$\begin{aligned} \min_{\mathbf{x}} \quad & \mathbf{c}'\mathbf{x} \\ s.t. \quad & \mathbf{A}\mathbf{x} = \mathbf{b} \\ & \mathbf{x} \geq \mathbf{0}, \end{aligned}$$

with $\mathbf{x} = (\mathbf{f}^{(1)'}, \dots, \mathbf{f}^{(\Lambda)'}, t_1, \dots, t_{|\mathcal{A}|})'$ and

$$\mathbf{A} = \left(\begin{array}{ccc|c} \mathbf{H} & & & \\ & \ddots & & \\ & & \mathbf{H} & \\ -\mathbf{I}_{|\mathcal{L}|} & \cdots & -\mathbf{I}_{|\mathcal{L}|} & \mathbf{R} \\ \hline & & & \mathbf{1}_{1 \times |\mathcal{A}|} \end{array} \right)$$

$$\mathbf{b} = (\mathbf{q}^{(1)'}, \dots, \mathbf{q}^{(\Lambda)'}, \mathbf{0}_{1 \times |\mathcal{L}|}, \mathbf{1})'$$

$$\mathbf{c} = \left(\mathbf{0}_{1 \times (|\mathcal{L}|\Lambda)}, \sum_{l \in \mathcal{L}} p_{l,1}, \dots, \sum_{l \in \mathcal{L}} p_{l,|\mathcal{A}|} \right)'$$

where \mathbf{R} is the $|\mathcal{L}| \times |\mathcal{A}|$ link capacity matrix with entries $r_{l,\alpha}$. Notice that the non-zero entries in \mathbf{c} correspond to the energy consumption of TPs.

Remark 1. Although there are some standard algorithms for solving LPs, e.g., Ellipsoid and simplex, to run such algorithms requires complete information of the constraint matrix A . In our case, such algorithms may become infeasible due to the practical difficulty in preparing the matrix A in advance. It is impractical, in either computation time or storage space, to list all those transmission patterns in advance. Without the constraint matrix A in advance, standard algorithms such as simplex, interior point, and ellipsoid method cannot be applied to solve the problem.

Remark 2. The number of patterns grows exponentially with the number of links (i.e., tuple-links) in the network, leading to exponentially many columns in the constraint matrix A . In this sense, the LP formulation does not change the NP-hard nature of the wireless network scheduling problem, but can allow the convenience to design efficient approximation algorithms.

4 DECOMPOSITION FRAMEWORK

In this section, we develop a decomposed method to iteratively solve Problem 1. All the problems rendered in the decomposition process are summarized in Table 2 and illustrated in Fig. 2.

3. The physical meaning of Lemma 1 is that whenever there is an over-scheduled link l , we can always adjust the scheduling to remove the redundant capacity by averaging out the traffic load from a current pattern to others with smaller capacity on l .

TABLE 2
Summarization of Optimization Problems

	Problem 1	Problem 2	Problem 3	Problem 3R
Description	original problem	master problem	sub-problem	relaxed sub-problem
Complexity (original)	$ \mathcal{P} ^{ \mathcal{L} } \approx \mathcal{P} ^{(\mathcal{V} ^2 \cdot \mathcal{R}_v ^2 \cdot \mathcal{L})}$	NA	$ \mathcal{L} ^2 \mathcal{P} ^{ \mathcal{L} }$	NA
Optimal solution	E^*	$E^{(k)}$	U^*	\tilde{U}
Proposed solution	\tilde{E}	$E^{(k)}$	\tilde{U}	\tilde{U}
Algorithm	Algorithm 2	any LP algorithm	Algorithm 1	Algorithm 3
Complexity (proposed)	iterative with LP	LP with moderate size	$ \mathcal{P} \mathcal{L} ^3$	$ \mathcal{R} $
Bound	lower bounded (Theorem 1)	optimally solved	upper bounded (Theorem 2 and 3)	optimally solved

Intuitively, not all the TPs will contribute to flow delivery and there is no need to allocate transmission time to TPs with little contribution. Our experiments in tuple-link scheduling [6], [9] also indicate that only a subset of \mathcal{A} will be scheduled. In other words, instead of considering all the patterns in \mathcal{A} , we only need to find and schedule the critical ones. To this end, we develop a decomposition technique based on delayed column generation [9] to iteratively find such a subset of critical TPs.

4.1 DCG-Based Decomposition

According to the matrix form of Problem 1, the size of the left half of constraint matrix \mathbf{A} is determined by the network topology, while each column in the right half corresponds to a TP. Therefore the number of scheduled TPs is equal to the number of columns in the right half of \mathbf{A} . Starting from an initial feasible solution obtained from a small subset of \mathcal{A} , the DCG method iteratively searches for new columns (or equivalently TPs) that are promising in improving the objective.

Let $\mathcal{A}^{(k)}$ denote the subset of TPs already found at the beginning of Step k . In Step k , the optimal solution with given $\mathcal{A}^{(k)}$ can be obtained by solving the following master problem:

Problem 2 (Master Problem).

$$\min_{\{f_l^{(\lambda)}, t_\alpha\}} E^{(k)} = \sum_{\alpha \in \mathcal{A}^{(k)}} \left(\sum_{l \in \mathcal{L}} p_{l,\alpha} \right) t_\alpha, \quad (13)$$

$$s.t. \quad f_l = \sum_{\lambda \in \Lambda} f_l^{(\lambda)} = \sum_{\alpha \in \mathcal{A}^{(k)}} r_{l,\alpha} t_\alpha \quad \forall l \in \mathcal{L} \quad (14)$$

$$\sum_{\alpha \in \mathcal{A}^{(k)}} t_\alpha = 1 \quad (15)$$

$$t_\alpha \geq 0, \quad \forall \alpha \in \mathcal{A}^{(k)} \quad (16)$$

constraints (3), (8).

Or in matrix form,

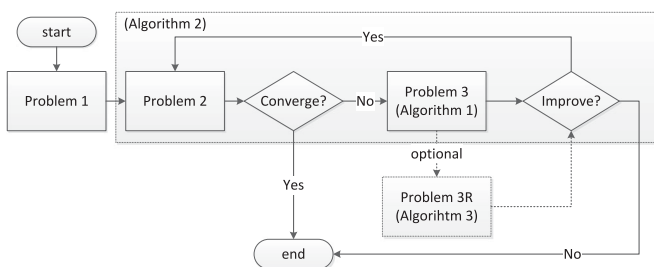


Fig. 2. Flowchart of the proposed joint optimization framework.

Problem 2 (Master problem in matrix form).

$$\begin{aligned} \min_{\mathbf{x}^{(k)}} \quad & \mathbf{c}^{(k)'} \mathbf{x}^{(k)} \\ s.t. \quad & \mathbf{A}^{(k)} \mathbf{x}^{(k)} = \mathbf{b} \\ & \mathbf{x}^{(k)} \geq \mathbf{0}, \end{aligned}$$

where $\mathbf{c} = (\mathbf{0}_{1 \times (|\mathcal{L}|\Lambda)}, \sum_{l \in \mathcal{L}} p_{l,1}, \dots, \sum_{l \in \mathcal{L}} p_{l,|\mathcal{A}^{(k)}|})$ and $\mathbf{x} = (\mathbf{f}^{(1)'}, \dots, \mathbf{f}^{(\Lambda)'}, t_1, \dots, t_{|\mathcal{A}^{(k)}|})'$. In the master problem, $\mathbf{A}^{(k)}$ has the same number of rows as \mathbf{A} but much fewer columns than \mathbf{A} .

The above master problem can be easily solved if the subset $\mathcal{A}^{(k)}$ is of moderate size. The solution of the master problem provides the scheduling time $t_\alpha^{(k)}$ for each pattern α in $\mathcal{A}^{(k)}$ along with the dual variable vector $\mathbf{w}^{(k)}$ associated with the constraints (where $\mathbf{w}^{(k)}$ is obtained by solving the dual problem of Problem 2). The next problem is to search for a new column \mathbf{A}_i to be added into $\mathcal{A}^{(k)}$ to generate $\mathcal{A}^{(k+1)}$, which can improve the objective of the optimization problem. In DCG algorithm, such an improvement is evaluated by the reduced cost $c_i - \mathbf{w}^{(k)'} \mathbf{A}_i$ where i denotes the index of the new column [34]. If a column is associated with negative reduced cost, then adding this column will improve the objective value.

Since the added columns only correspond to the right half of constraint matrix, it can be observed that adding a column is equivalent to adding a new pattern α , whose improvement⁴ can be evaluated as

$$= 0 + \sum_{l \in \mathcal{L}} w_l^{(k)} r_{l,\alpha} + w_0^{(k)} \times 1 - \sum_{l \in \mathcal{L}} p_{l,\alpha} \quad (17)$$

$$= \sum_{l \in \mathcal{L}} (w_l^{(k)} r_{l,\alpha} - p_{l,\alpha}) + w_0^{(k)}, \quad (18)$$

where $w_l^{(k)}$ is the dual variable corresponding to the l 'th row of matrix $\mathbf{R}^{(k)}$ in $\mathbf{A}^{(k)}$ (entry $r_{l,\alpha}$) and $w_0^{(k)}$ is the dual variable associated with the last row of \mathbf{A} .

Define the term $w_l^{(k)} r_{l,\alpha} - p_{l,\alpha}$ as the *utility* of link l in pattern α , and the utility sum of all the links as *system utility* $U^{(k)}$. The utility of each link consists of the contribution to flow traffic and the power cost, where the flow contribution of a link is further determined by both the link capacity $r_{l,\alpha}$ and the dual variable $w_l^{(k)}$. The expression of utility function $w_l^{(k)} r_{l,\alpha} - p_{l,\alpha}$ indicates that it should have the same unit as $p_{l,\alpha}$, which is power, while $w_l^{(k)}$ acts as a price factor to convert throughput into welfare.

4. We use the additive inverse of reduced cost as a measurement of the performance improvement to keep consistency with the later definition of utility.

A new TP will be added to $\mathcal{A}^{(k)}$ if it maximizes the improvement in (18). Since $w_0^{(k)}$ is a constant independent of the TP to be added in Step k for a given $\mathcal{A}^{(k)}$, it can be ignored during pattern selection. Then selecting a new TP is equivalent to solving the following problem:

Problem 3 (Sub-Problem).

$$\max_{\alpha \in \mathcal{A} \setminus \mathcal{A}^{(k)}} U_{\alpha}^{(k)} = \sum_{l \in \mathcal{L}} \left(w_l^{(k)} r_{l,\alpha} - p_{l,\alpha} \right). \quad (19)$$

Since energy efficiency is a compound of both the benefit in flow contribution and cost in power consumption, the expression in (19) naturally provides an evaluation function of a TP with these considerations. Therefore, the sub-problem can be interpreted as to search for the most energy-efficient TP, which is evaluated by the corresponding system utility. As mentioned previously, the system utility shares the same unit as that of power, which indicates that the objectives in sub-problem and original problem are consistent in unit. The new TP, if found, is then added to $\mathcal{A}^{(k)}$ to form $\mathcal{A}^{(k+1)}$. The master problem is then updated and solved to provide a new set of solutions. The process is repeated until no improvement can be made (or no column can be added), i.e., $\mathbf{w}^{(k)'} \mathbf{A}_i - c_i \leq 0, \forall i$. Then, the standard DCG theory shows that the current solution will be the optimal solution of Problem 1 [34].

The physical meaning behind the DCG decomposition can be explained as follows. We search for energy efficient TPs to perform scheduling, where the energy efficiency of TPs depends on the information obtained from current solution. Each time solving the master problem will provide an updated evaluation on all the links regarding their capabilities in satisfying traffic demand based on their performance in existing TPs, and such an evaluation is conveyed through dual variables $w_l^{(k)}$. Then according to this evaluation, the most energy efficient TP that can maximize the system utility is searched and fed back to the master problem. With this new information, links will be re-evaluated through solving the updated master problem. Repeating these steps will provide more and more accurate evaluations on the energy efficiency of TPs and therefore approach the optimal solution.

According to the definition of TP, finding a TP is equivalent to finding a power allocation over all the links. In this sense, the proposed framework can be interpreted as decomposing the original problem into scheduling phase (master problem) and power allocation phase (sub-problem). Optimality remains intact during the decomposition process by iteratively solving the two phases. Thus, with the multi-dimensional modeling, TP based scheduling and DCG based decomposition, the joint optimal solution over all dimensions of network resources can be obtained.

4.2 Initial Solution

It is usually difficult to find an initial subset of \mathcal{A} that can yield feasible solution. However, even if the initial solution is infeasible, we can still find new columns based on the dual variables, and the newly added columns can potentially drive the iteration to yield a feasible solution. Thus, even starting from an infeasible solution, the feasibility will be restored in several rounds, providing that the original Problem 1 is feasible. Based on this, the initial subset can be constructed with randomly selected TPs. However, if a link

is not included in the initial subset, then the link will probably never be evaluated or involved into the problem. Taken this issue into consideration, we need to cover every link in the initial subset. In addition, the constraint matrix should have full row rank [34]. Based on these, the initial subset can be set by choosing $|\mathcal{L}|$ TPs where each TP has exactly one unique link activated. In this way, we can get a diagonal matrix \mathbf{R} and matrix \mathbf{A} will have full row rank.

Remark 3. Theoretically, if the sub-problem can be solved optimally, the iterative process of DCG method will finally converge to the optimal solution of Problem 1 [34]. In our model, the sub-problem is to find a TP with maximum utility, which is done by searching over all the unused patterns. Again, due to the large size of TPs in the network ($|\mathcal{A}|$), it becomes computationally impractical to search over all the patterns to obtain the optimal solution. Therefore, we propose a light-weight greedy algorithm to approximately solve the sub-problem.

4.3 Greedy Algorithm for Solving the Sub-Problem

As previously mentioned, a TP is defined as a power allocation on all the links, therefore it is equivalent to finding an optimal power allocation on links to maximize the system utility (the superscript indicating number of rounds is omitted in this section since the sub-problem is solved within one round)

$$\max_{\{p_l\}} U = \sum_{l \in \mathcal{L}} u_l = \sum_{l \in \mathcal{L}} w_l r_l - p_l. \quad (20)$$

Power allocation on links with the objective of maximizing system utility is a challenging problem since the utilities of links are mutually dependent. Even if the utility of each link is fixed, the problem is still NP hard (which can be viewed as a maximum weighted independent set problem under physical interference model as in [11]). To obtain a practically feasible solution, we develop a greedy algorithm to find the optimal power allocation.

The greedy power allocation is done by starting with all-zero power allocation and gradually activating (assigning positive power levels to) links until the system utility no longer increases. Whether an inactive link can be activated depends on its contribution to the system utility. Among all the inactive links, the one with the largest contribution will be activated.

The details of the greedy algorithm are shown in Algorithm 1. Denote the set of active links and inactive links as \mathcal{S}_a and \mathcal{S}_i , respectively. At each step, the algorithm evaluates all the inactive links and selects one into the active set. According to Eq. (1) and the definition of utility, the utility of each link can be written as a function of its transmit power p_l and active link set \mathcal{S}

$$\begin{aligned} u_l &= u_l(p_l, \mathcal{S}) \\ &= w_l r_l - p_l \\ &= w_l B_l \log_2 \left(1 + \frac{g_l p_l}{\sum_{m \in \mathcal{S} \setminus \{l\}} g_m p_m + \sigma^2} \right) - p_l. \end{aligned} \quad (21)$$

Each inactive link first calculates a myopic optimal power level \hat{p}_l that maximizes its own utility assuming that the power levels of all the other links keep unchanged. \hat{p}_l can be obtained by calculating the utilities at all possible power

levels and choosing the one that gives maximum utility. Then it calculates the change of system utility ΔU_l if it is activated by using power \hat{p}_l

$$\Delta U_l = u_l(\hat{p}_l, \mathcal{S}_a) + \sum_{m \in \mathcal{S}_a} u_m(p_m, \mathcal{S}_a \cup \{l\}) - \sum_{m \in \mathcal{S}_a} u_m(p_m, \mathcal{S}_a), \quad (22)$$

i.e., ΔU_l can be viewed as the contribution of l if activated. For the link with the largest contribution, if its contribution is larger than a pre-defined non-negative constant ϵ ,⁵ it means activating this link can increase the system utility and this link will be activated at the calculated power level \hat{p}_l . Otherwise, the system utility cannot be increased and the algorithm stops. At the end of the algorithm, it outputs the power allocation to all links.

Algorithm 1. Greedy Algorithm for Problem 3

Input: dual variables $\{w_l\}_{l=1, \dots, |\mathcal{L}|}$;
Initialization: $p_l = 0, \forall l \in \mathcal{L}; \mathcal{S}_a = \emptyset; \mathcal{S}_i = \mathcal{L}; \hat{U} = 0$;
while $\mathcal{S}_i \neq \emptyset$ **do**
 for $l \in \mathcal{S}_i$ **do**
 $\hat{p}_l = \arg \max u_l(p_l, \mathcal{S}_a)$;
 Calculate ΔU_l according to Eq. (22);
 end
 $l^* = \arg \max_{l \in \mathcal{S}_i} \Delta U_l$ (If the solution is not unique, randomly select one link with $\max_{l \in \mathcal{S}_i} \Delta U_l$);
 if $\Delta U_{l^*} > \epsilon$ **then**
 move l^* from \mathcal{S}_i to \mathcal{S}_a ; $p_{l^*} = \hat{p}_{l^*}$;
 $\hat{U} = \hat{U} + \Delta U_{l^*}$;
 else
 Algorithm stops;
 end
end
Output: \hat{U} as the solution of Problem 3;
The corresponding power allocation $\{p_l\}_{l=1, \dots, |\mathcal{L}|}$.

4.4 Complexity Analysis

Each utility computation (as in Eq. (21)) incurs a complexity in the order of $|\mathcal{S}_a|$. Within each iteration of the greedy algorithm, each inactive link in \mathcal{S}_i will perform $|\mathcal{P}|$ utility computations to find the optimal power level and at most $2|\mathcal{S}_a|$ utility computations (as in Eq. (22)) to calculate the effect on other links. As a result, each iteration requires a total number of $(|\mathcal{P}| + 2|\mathcal{S}_a|)|\mathcal{S}_i||\mathcal{S}_a|$ computations to evaluate the contributions of all the inactive links, plus $|\mathcal{L}|$ computations to perform sorting. The iteration will be repeated by $|\mathcal{S}_a|$ times, leading to a total complexity of $[(|\mathcal{P}| + 2|\mathcal{S}_a|)|\mathcal{S}_i||\mathcal{S}_a| + |\mathcal{L}|]|\mathcal{S}_a|$.

In practice, there can be at most $|\mathcal{R}|/2$ links actived simultaneously due to radio conflict. Therefore in the result of the algorithm we will have $|\mathcal{S}_a| \leq |\mathcal{R}|/2$. In addition, $|\mathcal{S}_i| \leq |\mathcal{L}|$. Based on this, the computation complexity is in the order of $(|\mathcal{R}| + |\mathcal{P}|)|\mathcal{R}|^2|\mathcal{L}|$. Further, $|\mathcal{R}|$ is usually less than $|\mathcal{L}|$. Therefore the greedy algorithm's complexity will be in the order of $|\mathcal{P}||\mathcal{L}|^3$.

Since the number of TPs is $|\mathcal{P}|^{|\mathcal{L}|}$ and the complexity of calculating system utility of each TP is $|\mathcal{L}|^2$, the complexity of brute force searching over the entire space to find maximum utility TP is $|\mathcal{L}|^2|\mathcal{P}|^{|\mathcal{L}|}$, which is significantly higher than that by Algorithm 1.

5. ϵ can be set to 0, or positive if we want to terminate the algorithm earlier when the contribution of adding a new link is very small.

4.5 Algorithm Design

With the decomposition framework and the greedy algorithm, we can now design the decomposition algorithm for solving the original problem, as shown in Algorithm 2.

Algorithm 2. Decomposition Algorithm for Problem 1

Initial transmission pattern set $\mathcal{A}^{(0)}$;
 $k=0$;
while $E^{(k)} < E^{(k-1)}$ **do**
 //Master stage:
 Update master problem (Problem 2) with current TPs $\mathcal{A}^{(k)}$;
 Solve master problem to obtain energy $E^{(k)}$ and dual variables $\mathbf{w}^{(k)}$;
 //Sub-problem stage:
 Solve the sub-problem (Problem 3) using Algorithm 1 to obtain a new TP α (with the power allocation) and \hat{U} (to calculate performance bound);
 if $\mathbf{w}^{(k)\top} \mathbf{A}_\alpha - c_\alpha > 0$ **then**
 Add the new TP to $\mathcal{A}^{(k)}$ and obtain $\mathcal{A}^{(k+1)}$;
 $k \leftarrow k + 1$;
 Go to master stage;
 else
 break;
 end
end
 $\hat{E} = E^{(k)}$;
Output: \hat{E} as the approximate solution of Problem 1.

In the proposed framework, both the problem formulation and the proposed algorithms involve global information of the network such as the link states and power allocation. Therefore, a central agent is required to collect the information and perform the optimization computation, and a centralized approach is taken to develop algorithms in this paper. However, the ideas behind the proposed algorithms, such as the framework for jointly optimizing different types of network resources, the corresponding decomposition scheme to tackle the complexity issue, and the interplay between different network dimensions and the optimization, can be combined or incorporated with other approaches to efficiently solve optimization problems in various scenarios. For example, the concept of transmission patterns can be adopted in online scheduling algorithms for joint scheduling and power allocation in a dynamic network, and the decomposition approach can be combined with distributed algorithms to further reduce the complexity. We leave these investigations for our future work.

5 PERFORMANCE ANALYSIS

It is known that, theoretically, the DCG-based iterative algorithm will converge to an optimal solution of the original problem, providing that the sub-problem is optimally solved in every step [34]. Therefore, in our case, the optimality of the obtained solution is determined by that of the sub-problem. Below, we will first show how the performance of the greedy algorithm affects that of the original problem (Problem 1).

5.1 Performance of the Original Problem Solution

Denote the corresponding objectives achievable optimal solutions of the original problem (Problem 1) and the sub-problem (Problem 3) as E^* and U^* , respectively. When

Algorithm 2 stops, let the solution of the sub-problem solved by the greedy algorithm be \hat{U} , and the corresponding solution to Algorithm 2 be \hat{E} . Then we have the following relationship:

Theorem 1. *The performance gap of Algorithm 2 in solving the original problem is upper bounded by that of Algorithm 1 in solving the sub-problem, i.e.,*

$$\Delta_E = \hat{E} - E^* \leq U^* - \hat{U} = \Delta_U. \quad (23)$$

For the original problem, suppose the dual vector associated with \hat{E} is $\hat{\mathbf{w}}$, whose last entry is \hat{w}_0 . Before proving Theorem 1, we first present the following result.

Lemma 2. *If $\hat{\mathbf{w}}$'s last entry (\hat{w}_0) is replaced by $\hat{w}_0 - \Delta_U$, the resulting vector, denoted as $\tilde{\mathbf{w}}$, will still be a feasible solution to Problem 1's dual problem.*

Proof. Denote the dual problem of Problem 1 as:

Problem 1D (dual of Problem 1)

$$\begin{aligned} \max_{\mathbf{w}} \quad & \mathbf{w}'\mathbf{b} \\ \text{s.t.} \quad & \mathbf{w}'\mathbf{A} \leq \mathbf{c}'. \end{aligned}$$

Denote \mathbf{A}_i as a column of \mathbf{A} . For the columns in the left half of \mathbf{A} , replacing \hat{w}_0 with $\hat{w}_0 - \Delta_U$ will not affect the value of $\tilde{\mathbf{w}}'\mathbf{A}_i$ since the last row of left half of \mathbf{A} only has zero entries. Therefore, for these columns, $\tilde{\mathbf{w}}'\mathbf{A}_i \leq c_i$ still holds.

Recalling that each column of the right half of \mathbf{A} is associated with a TP, we can write Eq. (18) as $\mathbf{w}'\mathbf{A}_\alpha - c_\alpha = U_\alpha + \hat{w}_0$, where U_α is the system utility achieved by pattern α .

Since the decomposition algorithm stops at \hat{U} , we have

$$\begin{aligned} \hat{U} + \hat{w}_0 &= \hat{\mathbf{w}}'\mathbf{A}_\alpha - c_\alpha \leq 0 \\ \hat{w}_0 - \Delta_U &\leq -U^*. \end{aligned}$$

For $\tilde{\mathbf{w}}$ and every column in the right half of \mathbf{A} , we have

$$\begin{aligned} \tilde{\mathbf{w}}'\mathbf{A}_\alpha - c_\alpha &= U_\alpha + \hat{w}_0 - \Delta_U \\ &\leq U_\alpha - U^* \\ &\leq 0. \end{aligned}$$

Above all, $\tilde{\mathbf{w}}$ is a feasible solution to Problem 3. \square

Then we continue to prove Theorem 1.

Proof. Suppose \mathbf{x}^* and \mathbf{w}^* are the optimal solutions of the original problem (Problem 1) and its dual problem (Problem 1D), respectively. From Lemma 2, $\tilde{\mathbf{w}}$ is a feasible solution to Problem 1D. Therefore

$$\mathbf{w}^{*\prime}\mathbf{b} \geq \tilde{\mathbf{w}}'\mathbf{b} = \hat{\mathbf{w}}'\mathbf{b} - \Delta_U = \hat{E} - \Delta_U.$$

According to weak duality, $\mathbf{c}\mathbf{x}^* \geq \mathbf{w}^{*\prime}\mathbf{b}$, which leads to

$$\begin{aligned} \hat{E} - E^* &= \hat{E} - \mathbf{c}\mathbf{x}^* \leq \hat{E} - \mathbf{w}^{*\prime}\mathbf{b} \\ &\leq \hat{E} - (\hat{E} - \Delta_U) \\ &= \Delta_U. \end{aligned}$$

thus completing the proof of Theorem 1. \square

As discussed in Section 4.1, it can be observed that both performance gaps of the solutions of original problem and sub-problem are in the unit of power, which shows the

consistency of unit in Theorem 1. Moreover, Theorem 1 shows that the performance gap of the original optimization problems solution is bounded by that of the sub-problem. Therefore, the performance of the decomposition algorithm can be evaluated through investigating the performance gap of Algorithm 1 in solving the sub-problem.

5.2 Performance of the Sub-Problem Solution

The objective of the sub-problem is the system utility, whose maximum value is related to how many links can be activated simultaneously. Due to radio conflict, links sharing the same radio will not be activated at the same time, otherwise both of them will result in 0 utility. Considering that the tuple-link based multi-dimensional network model can be abstracted as a graph with radios being vertices and links being edges, the maximum number of concurrent links with positive utility can be characterized by the matching number of the graph associated with the network. Let M^* denote the matching number of the network. We have the following statement.

Lemma 3. *In the optimal solution of the sub-problem, there can be at most M^* links with positive utility.*

The proof of Lemma 3 follows directly the definition of matching number of graph.

Define $\tilde{u}_l = u_l(\hat{p}_l, \emptyset)$ as the *utopian utility* of a link, which is its optimal utility when ignoring any mutual interference. Notice that utopian utility is also the utility of each link in the first round of the greedy algorithm (Algorithm 1), and will not be smaller than the practically achieved utility when the corresponding link is scheduled. Without loss of generality, suppose $\{\tilde{u}_l\}$ is sorted in descending order, i.e., $\tilde{u}_1 > \tilde{u}_2 > \dots$. Based on this, we can derive one performance bound of Algorithm 1 as

Lemma 4.

$$\frac{\hat{U}}{U^*} \geq \frac{\tilde{u}_1}{\sum_{l=1}^{M^*} \tilde{u}_l} \geq \frac{1}{M^*}. \quad (24)$$

Proof. According to Algorithm 1, the system utility will be increased every time a new link is added, therefore the final system utility of the greedy algorithm \hat{U} will not be smaller than that in the first round, i.e., $\hat{U} \geq \tilde{u}_1$. On the other hand, there can be at most M^* links with positive utility according to Lemma 3. Hence, $U^* \leq \sum_{l=1}^{M^*} \tilde{u}_l$. Together we have

$$\frac{\hat{U}}{U^*} \geq \frac{\tilde{u}_1}{\sum_{l=1}^{M^*} \tilde{u}_l} \geq \frac{\tilde{u}_1}{M^* \tilde{u}_1} = \frac{1}{M^*}. \quad \square$$

Lemma 4 shows that the performance of the greedy algorithm is constant-bounded, and implies two ways of evaluating performance gap Δ_U , which are shown in the following theorem.

Theorem 2. *The performance gap of Algorithm 1 in solving sub-problem is upper bounded as*

$$\Delta_U \leq \sum_{l=2}^{M^*} \tilde{u}_l \quad (25)$$

$$\leq (M^* - 1)\hat{U}. \quad (26)$$

5.3 Bound from Sub-Problem Relaxation

For a given \hat{U} , estimating the upper bound of Δ_U is equivalent to estimating the upper bound of U^* . An upper bound of U^* can be obtained by solving a relaxed version of Problem 3 as follows.

The problem can be relaxed by ignoring some interference without changing the formulation. In other words, the relaxation of Problem 3 can be done by reducing the values of g_{lm} 's. For example, one relaxation can be ignoring all the interference or radio conflict in the network (i.e., $g_{lm} = 0, \forall l, m \in \mathcal{L}$) but limiting the total number of active links to M^* . In this case, the utility of each link is independent of other links' activities and the optimal system utility is $\sum_{l=1}^{M^*} \tilde{u}_l$, which is an interpretation of the bound in Eq. (25). However, in this case, tuple-links associated with the same physical link usually have the same dual values (w_l), which means they tend to be activated simultaneously if mutual interference is ignored. As a result, in the solution of this relaxed optimization problem, many links share same radios, which is physically infeasible. Therefore, this relaxation may yield a loose bound.

In order to formulate a proper relaxed problem to characterize an upper bound of U^* , we tighten the above relaxation by adding back part of the radio conflict as constraints. This relaxation will ignore co-channel interference and modify the radio constraint as follows: There could be at most $\min\{\mathcal{R}_u, \mathcal{R}_v\}$ tuple-links activated on any physical link between node u and v , while the total number of active tuple-links in the network is limited by M^* . Denote the relaxed problem as *Problem 3R*. The solution of Problem 3R can be obtained by greedily picking $\{\tilde{u}_l\}$ as long as the above constraint is not violated, as summarized in Algorithm 3.

Algorithm 3. Solving Problem 3R

Input: $\{\tilde{u}_l\}$ (sorted in descending order);
Initialization:
 Number of selected tuple-links on each physical link $n_{uv} = 0, \forall u, v \in \mathcal{N}$;
Total Number of active tuple-links $n = 0$;
Total utility $\tilde{U} = 0$;
 $l = 1$;
while $n < M^*$ and $\tilde{u}_l > 0$ **do**
 Find l 's corresponding physical link uv ;
if $n_{uv} < \min\{\mathcal{R}_u, \mathcal{R}_v\}$ **then**
 Tuple-link l is activated; $n = n + 1$;
 $n_{uv} = n_{uv} + 1$;
 $\tilde{U} = \tilde{U} + \tilde{u}_l$;
end
 $l = l + 1$;
end
Output: \tilde{U} as the (optimal) solution of Problem 3R.

Lemma 5. *Algorithm 3 yields the optimal solution of Problem 3R.*

Proof. Since the constraint only applies to each physical link locally and there is no co-channel interference, the behavior of each physical link has no influence on other physical links. On the other hand, it can be observed that the greedy selection of the links associated with one physical link is locally optimal. As a result, combining the local optimal solutions of independent physical links will yield the global optimal solution. \square

Define the list of utopian utilities as utopian list $(\{\tilde{u}_l\}, l = 1, 2, \dots, \mathcal{L})$. In Algorithm 3, at most M^* utopian utilities are added to the final system utility. Notice that these added utilities may not be the first M^* ones (M^* largest ones) in the utopian list, since some might be excluded due to the constraint defined in Problem 3R. Then define the list of added utopian utilities associated with the selected links in Algorithm 3 as reduced utopian list $(\{\tilde{u}_l^R\}, l = 1, 2, \dots, M^*)$. From the previous analysis, it can be observed that each \tilde{u}_l^R will be no larger than the corresponding \tilde{u}_l at the same position in the list,⁶ that is

$$\tilde{u}_l^R \leq \tilde{u}_l, \forall 1 \leq l \leq M^*. \quad (27)$$

Denote the optimal solution of Problem 3R as \tilde{U} , then Theorem 3 directly follows:

Theorem 3. *The performance gap of Algorithm 1 in solving sub-problem is upper bounded as*

$$\Delta_U \leq \tilde{U} - \hat{U} \leq \sum_{l=2}^{M^*} \tilde{u}_l^R, \quad (28)$$

where \tilde{u}_l^R are the utilities from reduced utopian list.

Compared with (25) in Theorem 2, the right hand sides are the summations of the same number of entries, while each entry in that of Theorem 3 is no larger than that of Theorem 2 (as implied by (27)), therefore the bound in Theorem 3 is usually tighter.

Combining Theorem 3 with Theorem 1, we can obtain a performance gap for the original problem. The size of the gap depends on the performance of the greedy algorithm and the level of relaxation of Problem 3R. For the greedy algorithm, if the links are highly interfered by each other, then it is more likely that the myopic selection in the greedy algorithm will diverse from the global optimal result. In Problem 3R, most of the relaxation is done by eliminating co-channel interference, which means the relaxation is looser if the interference is intensified. Based on these, intuitively we can see that the theoretical gap will be larger in networks with higher interference intensity, and smaller in a relatively less crowded network.

6 NUMERICAL RESULTS

We consider a connected MR-MC network with 25 nodes randomly deployed in a 1000×1000 m² area, as shown in Fig. 3. Each node is equipped with one or multiple radio interfaces, and there are multiple channels available for all radios. The transmit power of each radio can take values on a logarithmic scale from 0 to p_{\max} . The parameter settings are listed in Table 3.

6.1 Iteration and Optimality

We first tested the proposed decomposition framework and greedy algorithm on several sample topologies. In order to compare the result with the optimal solution, we solve the relaxed problem (Problem 3R) as described in Section 5.3 and apply Theorem 1 to obtain the lower bound of the optimal solution.⁷ The result of the objective value of Problem 1

6. Here, the subscript l indicates the location in the list, not a link. That is, \tilde{u}_l^R and \tilde{u}_l are at the same location in the corresponding lists, but not necessarily belong to the same link.

7. Theoretically, the lower bound is obtained when the algorithm converges. However, since we solved the relaxed problem in every round, the intermediate results are also presented as lower bound.

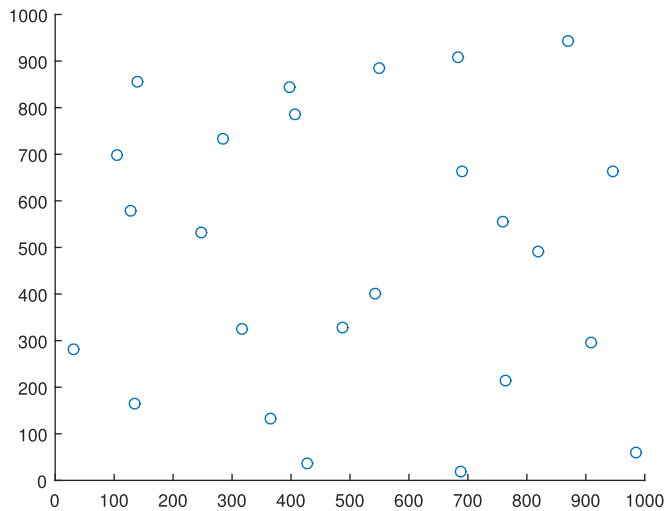


Fig. 3. Sample topology.

(energy consumption) and the corresponding lower bound of optimum (with intermediate results) are shown in Fig. 4. As shown in Fig. 4, when the result converges, there is a gap from the lower bound to the optimum. This gap naturally exists since the lower bound is calculated from the relaxed problem which ignores all co-channel interference and part of radio conflict. The optimal solution of the original problem will be worse (larger) than the lower bound, thus the actual distance between our solution and optimum will be smaller than the gap shown in the figures.

Remarks: The performance metrics used in the following, energy efficiency and computation time, are network specific. Therefore, we use numerical simulations based on a sample topology to demonstrate the effects of different parameters. Our simulations based on other topology showed that the general trends and observations hold. To avoid repeated presentations, we only show the results from one sample deployment.

6.2 Effect of Power Control

One of our major contributions in this paper is the joint scheduling and power control by applying more realistic physical interference model in multi-dimensional resource allocation. We compare the performance of the joint optimization with that without power control. Energy efficiency of the network is used as the performance metric, which is defined as the ratio of sum traffic demands of all commodities and total energy consumption (the objective function of Problem 1).

In order to demonstrate the effect on energy efficiency from joint optimization, we vary the number of available power levels and compare the achieved energy efficiency. Notice that when $|\mathcal{P}| = 2$, transmit power can only be either zero or maximum transmit power, which can be viewed as the solution without power control. The energy efficiency corresponding to different number of available power levels $|\mathcal{P}|$ is shown in Fig. 5. As can be seen from this figure, the proposed approach with power control ($|\mathcal{P}| > 2$) always outperforms that without power control. This is because when without power control, whenever a link is scheduled for transmission, the maximum transmit power is used, which might be unnecessarily high and generates high interference to other links. Especially when the traffic demand is low, allowing links to transmit at low power levels can be

TABLE 3
Parameter Setting

Parameter	Value (Default)
p_{\max}	10 mW
Maximum transmission range	250 m
Channel noise power	-30 dBm
Path loss factor	2
Flow demand	35 or 70 Kbps per flow
Number of radios	1-3 per node (2)
Number of channels	1-8 (4)
Bandwidth	1 Mbps

beneficial in improving energy efficiency. A more fine-grained power level set can also increase the number of TPs and hence facilitates better resource allocation to reduce mutual interference. Therefore involving power control into joint resource allocation can improve the network energy efficiency.

On the other hand, as illustrated in Fig. 5, further increasing the number of available power levels actually makes little difference to the network energy efficiency. For example, to meet a high traffic demand, links tend to use high transmit power in order to increase link capacity, leading to no use of low power levels. In view of the increased complexity of Algorithm 2 for more power levels, it is suggested to properly allocate the power level set according to the traffic demand level.

We further compare the results under various maximum transmit power p_{\max} for the radios. As shown in Fig. 6, without power control, we may observe a trend that the energy efficiency will decrease as p_{\max} increases. Similarly as previous discussion, when p_{\max} is increased, the fixed power case has to use higher power for transmission, leading to a degradation in energy efficiency. While in the case with power control, even if p_{\max} is increased, radios are still able to use low transmit power. As a result, the energy efficiency is almost unchanged when varying p_{\max} . In practice, if a large p_{\max} has to be chosen in order to satisfy high traffic demand, then taking power control into resource allocation can help maintain the energy efficiency of the network, which shows another benefit of joint resource allocation.

6.3 Sensitivity to Radio/Channel Resources

We further evaluate the performance of the proposed joint resource allocation under different network configurations and investigate the effect of different types of network resources on energy efficiency. The energy efficiency comparison under various numbers of radios and channels is shown in Fig. 7. The missing data points (e.g., there is no curve for high demand in Fig. 7a) is due to no feasible solution found after a large number of rounds (which likely means the original problem is infeasible).

In consistency with the previous section, it is observed that the result with power control can outperform that of fixed power (without power control) in all scenarios. As aforementioned, more choices of power levels enable transmissions with lower power when traffic demand is low, thus improving the network energy efficiency.

In Fig. 7, higher traffic demand often leads to lower energy efficiency. Generally, higher traffic demand requires more simultaneous transmissions or higher transmit power, which leads to more co-channel interference and

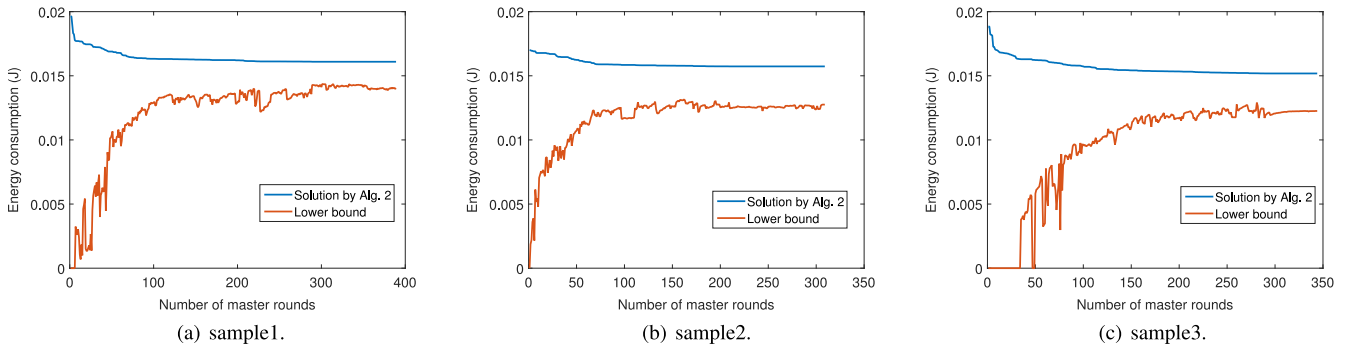


Fig. 4. Energy consumption of the proposed algorithm and the lower bound of optimum.

degradation of transmission quality as well as energy efficiency. Thus, a direct remedy can be exploiting more channel resources. As seen from Fig. 7, when more channels become available, the energy efficiency in the high demand case is not much less than that of low demand.

When there is only one or a few channels in the network, it is more likely that simultaneous transmissions will take place in the same channel and suffer co-channel interference, which will impact energy efficiency. While more channels means transmissions can be separated to different bands and avoid co-channel interference. However, more channels may not lead to better performance all the time, as can be seen in Fig. 7. When the number of channels is very large but the number of radios is limited, the extra spectrum resource cannot be fully utilized due to radio conflict. In other words, there are not enough radios to occupy these channel bands. Furthermore, there is no obvious performance improvement from 2 radios to 3 radios when the demand is low, which indicates that the one extra radio can be turned off or put to sleep mode to save energy.

These results may guide choosing proper numbers of radios or channels in the network. If the number of radios is given, choose the least number of channels that can maximize energy efficiency of the network. If the number of channels is given, turn on just enough number of radio interfaces and turn off the extra radios. In addition, the number of radios and channels can be jointly determined according to traffic demand to avoid excessive expenditure of resources. The results also suggest that there might exist some level of redundancy in the network resources in the

sense that not all the available radios, channels or power levels are necessary, and the optimal settings of these parameters are preferred such that the network performance can be optimized without oversizing the problem. Therefore, solving the joint resource allocation problems can reveal the knowledge of how many radios/channels/power levels will be actually used in obtaining the optimal solution, as a guidance for practical network deployment.

6.4 Trade-off between SE and EE

Spectrum efficiency (SE) is defined as the ratio of achieved data rate over spectrum resource (i.e., in this paper, the total bandwidth). Generally when EE increases, SE will decrease, and vice versa. Such a trade-off between SE and EE is shown in Figs. 8a and 8b. We also compare the corresponding spectrum-energy efficiency (SEE) in Fig. 8c, which is defined as SE divided by energy consumption.

Consider a simple example that if the bandwidth is doubled, then the transmission time of all the links can be halved while the traffic demand can still be satisfied but the energy consumption is halved. In this case, SE is halved and EE is doubled. This simplified analysis can explain the trends in Figs. 8a and 8b. However, the effect of bandwidth on EE is more than this. In the example, since the transmission time of all the links is halved, it means less simultaneous transmissions are required, which will potentially reduce co-channel interference and thus further improve energy efficiency. As a result, EE will be increased more than twice. Following this analysis, the trend in Fig. 8c can be explained that SEE will grow as the bandwidth increases.

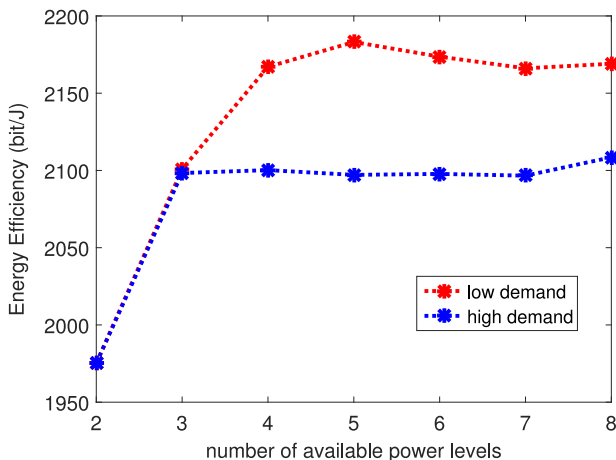


Fig. 5. Energy efficiency under different number of available power levels.

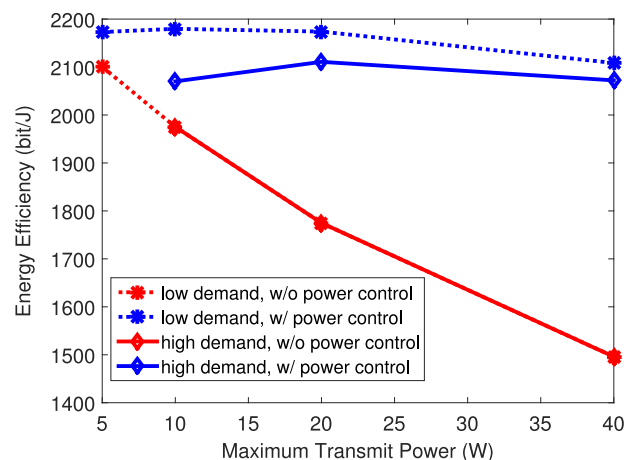


Fig. 6. Energy efficiency under different p_{\max} .

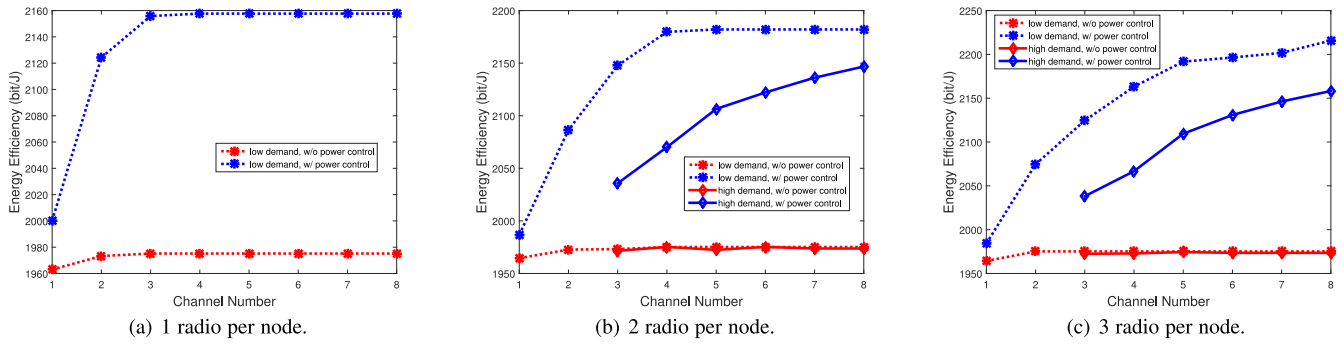


Fig. 7. Energy efficiency comparison under different network parameters.

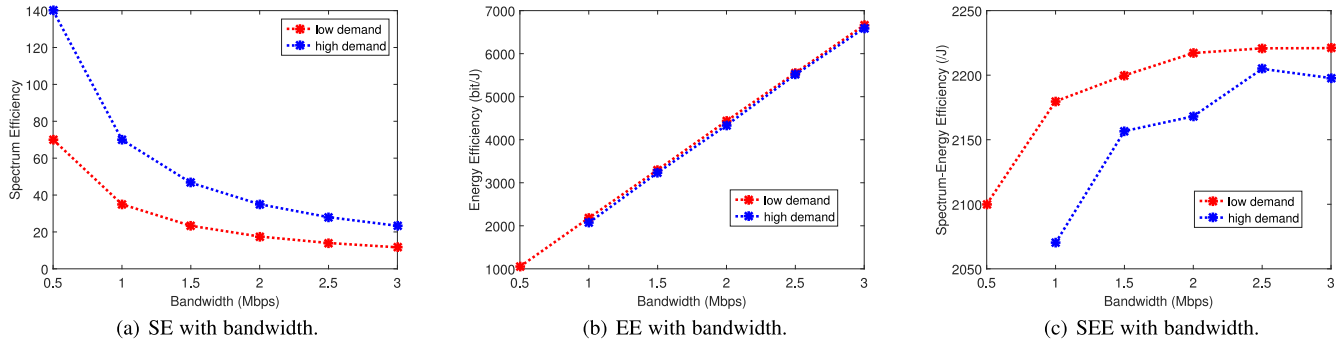


Fig. 8. SE and EE trade-off under different bandwidths.

6.5 Computation Time

The computation time of the decomposition algorithm is determined by the time consumption in each round and the number of rounds to converge, where the latter depends on the network topology and parameter setting. Even if the topology and parameters are the same, due to the randomness introduced from breaking tied values, the required number of rounds may also be different. Since the iterative process can be viewed as finding more accurate evaluation of TPs and finding better TPs based on the evaluation, the larger scale the network is, the more difficult in finding the final result. As a result, generally as the scale of network increases, it will take more rounds to converge as shown in Table 4.

Within each round, the computation mainly consists of two stages: the master stage of solving an LP problem and the sub-problem stage of a greedy algorithm. Table 4 shows the average computation time per round in the first 100 rounds for these two stages under different network configurations.

TABLE 4
Computation Time

configuration	rounds	master-time	sub-time
1-2-140	< 100	0.03s	0.03s
1-5-350	150 ~ 200	0.07s	0.08s
1-8-560	200 ~ 250	0.12s	0.14s
2-2-560	50 ~ 100	0.10s	0.16s
2-5-1400	200 ~ 300	0.27s	0.59s
2-8-2240	400 ~ 500	0.60s	1.39s
3-2-1260	200 ~ 300	0.21s	0.47s
3-5-3150	> 500	0.69s	2.01s
3-8-5040	> 1000	1.32s	4.67s

* (1-2-140 means 1 radio per node, totally two channels and 140 links).

The computation time of solving master problem is mainly determined by the size of the constraint matrix $\mathcal{A}^{(k)}$. In our case, the number of rows of $\mathcal{A}^{(k)}$ is equal to the number of links, and its number of columns is initialized also at the number of links but increased by one in each round. From the result we can observe that the computation time of master stage is almost linear with the number of links.

The time consumption in solving sub-problem with greedy algorithm also grows with the number of links. Within the greedy algorithm, links will be gradually activated until the total utility is maximized. The number of activated links or the number of rounds in greedy algorithm also affects the computation time. For example, in Table 4, the 3rd and 4th cases are both with 560 links, but the average time consumed in greedy algorithm for the 4th case is longer than that of the 3rd case. This is because in the 2-radio case, more links can be activated simultaneously and correspondingly the greedy algorithm will run more rounds to add these links.

6.6 Comparison with Random Algorithm

We further compare the performance of the proposed algorithm with a random pattern selection algorithm. The random algorithm takes the same initial pattern set as the proposed one, while the set is further augmented with randomly selected TPs, based on which a one-shot solution is obtained. In other words, the random algorithm solves Problem 2 with a TP set constructed by the initial set and added patterns. For the number of added patterns, we take a number equal to the number of patterns used in the proposed solution (labeled as “random-1”) and a number ten times of that (labeled as “random-10”) for comparisons. For example, if 100 patterns (additional to the initial ones) are selected in the proposed algorithm, then the random algorithm is run twice with 100 and 1,000 random selected

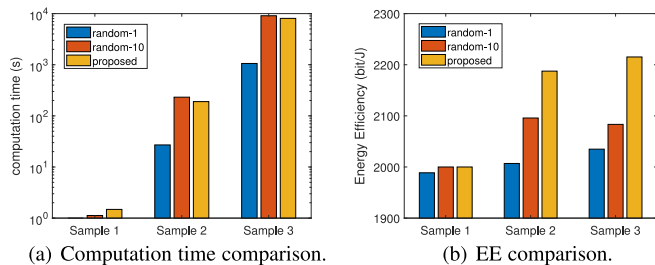


Fig. 9. Performance comparisons with random pattern selection algorithm.

patterns added, respectively. The performance comparisons on computation time and energy efficiency are shown in Fig. 9 under different network scenarios, with “Sample 1” for 1 radio and 1 channel, “Sample 2” for 2 radios and 4 channels, “Sample 3” for 3 radios and 8 channels.

For the comparison of computation time, the random algorithm shows its advantage since it is non-iterative and the optimization problem only needs to be solved once. The computation time is mainly spent in finding non-repeated patterns to be added to the problem. In terms of the achieved objective values, the random algorithm is always outperformed by the proposed algorithm, since the proposed algorithm selects patterns more “smart” in the sense that only patterns able to improve the objective value are selected. Especially, when the network dimension is high, in view of the huge number of possible patterns, it becomes less probable for the random selection to cover the really useful patterns. In this sense, the proposed algorithm scales well with the network dimensions since the patterns are selected based on utilities, which are the evaluations of the patterns potential contribution to the objective.

7 CONCLUSION

In this paper we have investigated energy-efficient joint resource allocation in generic wireless networks with multi-dimensional resource space. We have formulated a joint scheduling and power control problem which aims at minimizing energy consumption of the network while satisfying flow demand requirements. The large-scale problem with coupled variables has been solved efficiently by decomposition based on DCG method and greedy algorithm. The solution provides a joint allocation of radio, channel, transmit power as well as scheduling and routing. Theoretical analysis on the performance of the proposed algorithm has been conducted, and numerical results demonstrated that the proposed algorithm can improve energy efficiency of MR-MC networks with joint scheduling and power control.

ACKNOWLEDGMENTS

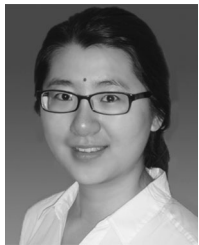
This work was supported in part by US National Science Foundation grant ECCS-1610874, and the National Natural Science Foundation of China under Grant 61628107, 61573103, 61861136003, 61571265, 91638204, and 61621091.

REFERENCES

- [1] M. Naeem, A. Anpalagan, M. Jaseemuddin, and D. C. Lee, “Resource allocation techniques in cooperative cognitive radio networks,” *IEEE Commun. Surveys Tuts.*, vol. 16, no. 2, pp. 729–744, Apr.–Jun. 2014.
- [2] I. W.-H. Ho, P. P. Lam, P. H. J. Chong, and S. C. Liew, “Harnessing the high bandwidth of multiradio multichannel 802.11n mesh networks,” *IEEE Trans. Mobile Comput.*, vol. 13, no. 2, pp. 448–456, Feb. 2014.

- [3] H. Li, Y. Cheng, C. Zhou, and P. Wan, “Multi-dimensional conflict graph based computing for optimal capacity in MR-MC wireless networks,” in *Proc. IEEE Int. Conf. Distrib. Comput. Syst.*, 2010, pp. 774–783.
- [4] J. Chen, Q. Yu, P. Cheng, Y. Sun, Y. Fan, and X. Shen, “Game theoretical approach for channel allocation in wireless sensor and actuator networks,” *IEEE Trans. Autom. Control*, vol. 56, no. 10, pp. 2332–2344, Oct. 2011.
- [5] A. Saifullah, Y. Xu, C. Lu, and Y. Chen, “Distributed channel allocation protocols for wireless sensor networks,” *IEEE Trans. Parallel Distrib. Syst.*, vol. 25, no. 9, pp. 2264–2274, Sep. 2014.
- [6] Y. Cheng, H. Li, D. M. Shila, and X. Cao, “A systematic study of maximal scheduling algorithms in multiradio multichannel wireless networks,” *IEEE/ACM Trans. Netw.*, vol. 23, no. 4, pp. 1342–1355, Aug. 2015.
- [7] H. Li, Y. Cheng, C. Zhou, and W. Zhuang, “Minimizing end-to-end delay: A novel routing metric for multi-radio wireless mesh networks,” in *Proc. IEEE INFOCOM*, 2009, pp. 46–54.
- [8] M. Li, S. Salinas, P. Li, X. Huang, Y. Fang, and S. Glisic, “Optimal scheduling for multi-radio multi-channel multi-hop cognitive cellular networks,” *IEEE Trans. Mobile Comput.*, vol. 14, no. 1, pp. 139–154, Jan. 2015.
- [9] Y. Cheng, X. Cao, X. S. Shen, D. M. Shila, and H. Li, “A systematic study of the delayed column generation method for optimizing wireless networks,” in *Proc. ACM Int. Symp. Mobile Ad Hoc Netw. Comput.*, 2014, pp. 23–32.
- [10] X. Cao, L. Liu, W. Shen, and Y. Cheng, “Distributed scheduling and delay-aware routing in multihop MR-MC wireless networks,” *IEEE Trans. Veh. Technol.*, vol. 65, no. 8, pp. 6330–6342, Aug. 2016.
- [11] P.-J. Wan, O. Frieder, X. Jia, F. Yao, X. Xu, and S. Tang, “Wireless link scheduling under physical interference model,” in *Proc. IEEE INFOCOM*, 2011, pp. 838–845.
- [12] Y. Zhou, Z. Li, M. Liu, Z. Li, S. Tang, X. Mao, and Q. Huang, “Distributed link scheduling for throughput maximization under physical interference model,” in *Proc. IEEE INFOCOM*, 2012, pp. 2691–2695.
- [13] L. B. Le, E. Modiano, C. Joo, and N. B. Shroff, “Longest-queue-first scheduling under SINR interference model,” in *Proc. ACM Int. Symp. Mobile Ad Hoc Netw. Comput.*, 2010, pp. 41–50.
- [14] A. Ephremides and T. V. Truong, “Scheduling broadcasts in multihop radio networks,” *IEEE Trans. Commun.*, vol. 38, no. 4, pp. 456–460, Apr. 1990.
- [15] G. Sharma, R. R. Mazumdar, and N. B. Shroff, “On the complexity of scheduling in wireless networks,” in *Proc. 12th Annu. Int. Conf. Mobile Comput. Netw.*, 2006, pp. 227–238.
- [16] C. Joo, X. Lin, J. Ryu, and N. B. Shroff, “Distributed greedy approximation to maximum weighted independent set for scheduling with fading channels,” *IEEE/ACM Trans. Netw.*, vol. 24, no. 3, pp. 1476–1488, Jun. 2016.
- [17] K. R. Malekshan and W. Zhuang, “Joint scheduling and transmission power control in wireless ad hoc networks,” *IEEE Trans. Wireless Commun.*, vol. 16, no. 9, pp. 5982–5993, Sep. 2017.
- [18] L. Liu, X. Cao, W. Shen, Y. Cheng, and L. Cai, “DAFEE: A decomposed approach for energy efficient networking in multi-radio multi-channel wireless networks,” in *Proc. IEEE INFOCOM*, 2016, pp. 1–9.
- [19] R. Xie, F. R. Yu, H. Ji, and Y. Li, “Energy-efficient resource allocation for heterogeneous cognitive radio networks with femtocells,” *IEEE Trans. Wireless Commun.*, vol. 11, no. 11, pp. 3910–3920, Nov. 2012.
- [20] L. Lu, D. He, Y. Xingxing, and G. Y. Li, “Energy-efficient resource allocation for cognitive radio networks,” in *Proc. IEEE Global Commun. Conf.*, 2013, pp. 1026–1031.
- [21] Q. Ni and C. C. Zarakovitis, “Nash bargaining game theoretic scheduling for joint channel and power allocation in cognitive radio systems,” *IEEE J. Sel. Areas Commun.*, vol. 30, no. 1, pp. 70–81, Jan. 2012.
- [22] S. Wang and C. Wang, “Joint optimization of spectrum and energy efficiency in cognitive radio networks,” *Digit. Commun. Netw.*, vol. 1, no. 3, pp. 161–170, 2015.
- [23] Z. Zhou, M. Dong, K. Ota, J. Wu, and T. Sato, “Distributed interference-aware energy-efficient resource allocation for device-to-device communications underlying cellular networks,” in *Proc. IEEE Global Commun. Conf.*, 2014, pp. 4454–4459.
- [24] F. Wang, C. Xu, L. Song, Q. Zhao, X. Wang, and Z. Han, “Energy-aware resource allocation for device-to-device underlay communication,” in *Proc. IEEE Int. Conf. Commun.*, 2013, pp. 6076–6080.

- [25] L. Liu, X. Cao, Y. Cheng, and L. Wang, "On optimizing energy efficiency in multi-radio multi-channel wireless networks," in *Proc. IEEE Global Commun. Conf.*, 2014, pp. 4436–4441.
- [26] L. Liu, X. Cao, Y. Cheng, L. Du, W. Song, and Y. Wang, "Energy-efficient capacity optimization in wireless networks," in *Proc. IEEE INFOCOM*, 2014, pp. 1384–1392.
- [27] E. Anderson, C. Phillips, D. Sicker, and D. Grunwald, "Optimization decomposition for scheduling and system configuration in wireless networks," *IEEE/ACM Trans. Netw.*, vol. 22, no. 1, pp. 271–284, Feb. 2014.
- [28] M. Sheng, C. Xu, X. Wang, Y. Zhang, W. Han, and J. Li, "Utility-based resource allocation for multi-channel decentralized networks," *IEEE Trans. Commun.*, vol. 62, no. 10, pp. 3610–3620, Oct. 2014.
- [29] K. K. Mensah, R. Chai, D. Bilibashi, and F. Gao, "Energy efficiency based joint cell selection and power allocation scheme for HetNets," *Digit. Commun. Netw.*, vol. 2, no. 4, pp. 184–190, 2016.
- [30] Y. Zhao, Y. Li, H. Zhang, N. Ge, and J. Lu, "Fundamental tradeoffs on energy-aware D2D communication underlying cellular networks: A dynamic graph approach," *IEEE J. Sel. Areas Commun.*, vol. 34, no. 4, pp. 864–882, Apr. 2016.
- [31] M. Li, P. Li, X. Huang, Y. Fang, and S. Glisic, "Energy consumption optimization for multihop cognitive cellular networks," *IEEE Trans. Mobile Comput.*, vol. 14, no. 2, pp. 358–372, Feb. 2015.
- [32] E. Oh, K. Son, and B. Krishnamachari, "Dynamic base station switching-on/off strategies for green cellular networks," *IEEE Trans. Wireless Commun.*, vol. 12, no. 5, pp. 2126–2136, May 2013.
- [33] S. Luo, R. Zhang, and T. J. Lim, "Downlink and uplink energy minimization through user association and beamforming in C-RAN," *IEEE Trans. Wireless Commun.*, vol. 14, no. 1, pp. 494–508, Jan. 2015.
- [34] D. Bertsimas and J. N. Tsitsiklis, *Introduction to Linear Optimization*. Belmont, MA, USA: Athena Scientific, 1997.

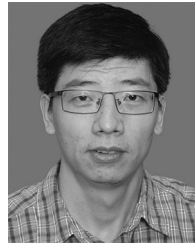


Lu Liu (S'13-M'18) received the PhD degree in computer engineering from the Illinois Institute of Technology, Chicago, Illinois, in 2017. Her current research interest includes energy efficient networking and communication, resource allocation and protocol design of wireless networks, and machine learning based network optimization. She is a member of the IEEE.



Yu Cheng (SM'09) received the BE and ME degrees in electronic engineering from Tsinghua University, in 1995 and 1998, respectively, and the PhD degree in electrical and computer engineering from the University of Waterloo, Canada, in 2003. He is now a full professor with the Department of Electrical and Computer Engineering, Illinois Institute of Technology. His research interests include wireless network performance analysis, network security, cloud computing, big data, integration of heterogeneous networks, and

machine learning. He received a Postdoctoral Fellowship Award from the Natural Sciences and Engineering Research Council of Canada (NSERC) in 2004, and a Best Paper Award from the conferences QShine 2007 and ICC 2011, and the Best Paper Runner-Up Award from ACM MobiHoc 2014. He received the National Science Foundation (NSF) Career Award in 2011 and IIT Sigma Xi Research Award in the junior faculty division in 2013. He served as a co-chair for the Wireless Networking Symposium of IEEE ICC 2009, a co-chair for the Communications QoS, Reliability, and Modeling Symposium of IEEE GLOBECOM 2011, a co-chair for the Signal Processing for Communications Symposium of IEEE ICC 2012, a co-chair for the Ad Hoc and Sensor Networking Symposium of IEEE GLOBECOM 2013, a co-chair for Communication and Information System Security Symposium of IEEE ICC 2016, and a technical program committee (TPC) co-chair for WASA 2011, ICNC 2015, and IEEE/CIC ICC 2015. He is a founding vice chair of the IEEE ComSoc Technical Subcommittee on Green Communications and Computing. He is an associated editor of the *IEEE Transactions on Vehicular Technology*. He was an IEEE ComSoc distinguished lecturer in 2016-2017. He is a senior member of the IEEE.



Xianghui Cao (S'08-M'11-SM'16) received the BS and PhD degrees both from Zhejiang University, Hangzhou, China, in 2006 and 2011, respectively. From 2012 to 2015, he was a senior research associate with the Illinois Institute of Technology, Chicago. He is currently an associate professor with Southeast University, Nanjing, China. His research interests include cyber-physical systems, wireless network performance analysis, wireless networked control, and network security. He serves/served as the organization chair for the 33rd Youth Academic Annual Conference of Chinese Association of Automation (YAC'18), publicity co-chair for ACM MobiHoc'15, symposium co-chair for ICNC'17 and IEEE/CIC ICC'15, and a TPC member for a number of conferences. He also serves as an associate editor for several journals, including *ACTA Automatica Sinica*, the *IEEE/CAA Journal of Automatica Sinica*, the *KSI Transactions on Internet and Information Systems*, and the *International Journal of Ad Hoc and Ubiquitous Computing*. He was a recipient of the Best Paper Runner-Up Award from ACM MobiHoc'14 and the first prize of the Natural Science Award by Ministry of Education, China. He is a senior member of the IEEE.



Sheng Zhou received the BE and PhD degrees in electronic engineering from Tsinghua University, Beijing, China, in 2005 and 2011, respectively. From January to June 2010, he was a visiting student with the Wireless System Lab, Department of Electrical Engineering, Stanford University, Stanford, California. From November 2014 to January 2015, he was a visiting researcher with the Central Research Lab of Hitachi Ltd., Japan. He is currently an associate professor with the Department of Electronic Engineering, Tsinghua University. His research interests include cross-layer design for multiple antenna systems, mobile edge computing, and green wireless communications. He is a member of the IEEE.



Zhisheng Niu received the graduate degree from Northern Jiaotong University (currently Beijing Jiaotong University), China, in 1985, and the ME and DE degrees from the Toyohashi University of Technology, Japan, in 1989 and 1992, respectively. During 1992-1994, he worked for Fujitsu Laboratories Ltd., Japan, and in 1994 joined Tsinghua University, Beijing, China, where he is now a professor with the Department of Electronic Engineering. He was a visiting researcher with the National Institute of Information and

Communication Technologies (NICT), Japan (10/1995-02/1996), Hitachi Central Research Laboratory, Japan (02/1997-02/1998), Saga University, Japan (01/2001-02/2001), Polytechnic University of New York, (01/2002-02/2002), University of Hamburg, Germany (09/2014-10/2014), and University of Southern California, (11/2014-12/2014). His major research interests include queueing theory, traffic engineering, mobile Internet, radio resource management of wireless networks, and green communication and networks. He has served as chair of the Emerging Technologies Committee (2014-2015), director for conference publications (2010-2011), and director for the Asia-Pacific Board (2008-2009) of the IEEE Communication Society, councilor of IEICE-Japan (2009-2011), and a member of the IEEE Teaching Award Committee (2014-2015) and IEICE Communication Society Fellow Evaluation Committee (2013-2014). He has also served as associate editor-in-chief of IEEE/CIC joint publication *China Communications* (2012-2016), editor of the *IEEE Wireless Communication* (2009-2013), editor of the *Wireless Networks* (2005-2009), and currently serving as an area editor of the *IEEE Transactions Green Communications & Networks* and director for online content of IEEE ComSoc (2018-2019). He has published more than 100 journal and more than 200 conference papers in IEEE and IEICE publications and co-received the Best Paper Awards from the 13th, 15th, and 19th Asia-Pacific Conference on Communication (APCC) in 2007, 2009, and 2013, respectively, International Conference on Wireless Communications and Signal Processing (WCSP13), and the Best Student Paper Award from the 25th International Teletraffic Congress (ITC25). He received the Outstanding Young Researcher Award from the Natural Science Foundation of China in 2009 and the Best Paper Award from the IEEE Communication Society Asia-Pacific Board in 2013. He was also selected as a distinguished lecturer of the IEEE Communication Society (2012-2015) as well as the IEEE Vehicular Technologies Society (2014-2016). He is a fellow of the IEEE and IEICE.



Ping Wang (M'08-SM'15) received the PhD degree in electrical engineering from the University of Waterloo, Canada, in 2008. She was with Nanyang Technological University, Singapore. She is currently an associate professor with the Department of Electrical Engineering and Computer Science, York University, Canada. Her current research interests include resource allocation in multimedia wireless networks, cloud computing, and smart grid. She was a co-recipient of the Best Paper Award from the IEEE International Conference on Communications in 2007 and the IEEE Wireless Communications and Networking Conference in 2012. She served as an editor of the *IEEE Transactions on Wireless Communications*, the *EURASIP Journal on Wireless Communications and Networking*, and the *International Journal of Ultra Wideband Communications and Systems*. She is a senior member of the IEEE.

► **For more information on this or any other computing topic, please visit our Digital Library at www.computer.org/publications/dlib.**